Chinese Chemical Letters 32 (2021) 2617–2628

Contents lists available at ScienceDirect

Chinese Chemical Letters

journal homepage: www.elsevier.com/locate/cclet

Review

Recent advances in kaolinite-based material for photocatalysts

Zhou Cao[a], Qizhao Wang[a,*], Hongfei Cheng[a,b,*]

[a] School of Water and Environment, Key Laboratory of Subsurface Hydrology and Ecological Effects in Arid Region of Ministry of Education, Chang'an University, Xi'an 710054, China
[b] Department of Materials Science and Engineering, Northwestern University, Evanston, IL, 60208, United States

ARTICLE INFO

Article history:
Received 31 October 2020
Received in revised form 2 December 2020
Accepted 28 December 2020
Available online 12 January 2021

Keywords:
Kaolinite
Titanium dioxide
Graphite carbonitride
Photocatalyst
Heterojunction

ABSTRACT

The composite catalytic materials based on the mineral kaolinite are considered to be a potential approach for solving global energy scarcity and environmental pollution, which have excellent catalytic performance, low cost and excellent chemical stability. However, pure kaolinite does not have visible light absorption ability and cannot be used as a potential photocatalytic material. Fortunately, the unique physical and chemical properties of kaolinite can be acted as a good semiconductor carrier. Herein, this paper firstly presents the mineralogical characteristics of kaolinite. Next, kaolinite-based photocatalysts (such as TiO_2/kaolinite, g-C_3N_4/kaolinite, g-C_3N_4/TiO_2/kaolinite, ZnO) are discussed in detail from the formation of heterostructures, synthesis-modification methods, photocatalytic mechanisms, and electron transfer pathways. Furthermore, the specific role of kaolinite in photocatalytic materials is summarized and discussed. In addition, the photocatalytic applications of kaolinite-based photocatalysts in the fields of water decomposition, pollutant degradation, bacterial disinfection are reviewed. However, the modification of kaolinite is hard, the manufacture of a large number of kaolinite-based photocatalysts is difficult, the cost of doping noble metals is expensive, and the utilization rate of visible light is low, which limits its application in industrial practice. Finally, this paper presents some perspectives on the future development of kaolinite-based photocatalysts.

1. Introduction

With the rapid development of economy and technology, the increasingly serious global energy shortage crisis and environmental pollution are becoming two major problems for the development of human society [1,2]. The research scholars spend a lot of effort to explore green environmental protection, economically sustainable technology to solve the above problems. Among many methods, photocatalytic degradation has many advantages such as economy, high efficiency, pollution-free and safety [3,4], which is an ideal solution to solve energy and environmental pollution problems. The photocatalytic reaction system uses inexhaustible sunlight as a driving force to directly convert the absorbed light energy into chemical energy or biochemical energy for practical application, such as hydrogen production from water splitting [5], degradation of organic pollutants in the environment [6], reduction of CO_2 to hydrocarbon fuel energy [7], photo-assisted traditional electrocatalytic application [8], and even disinfection of bacteria [9].

In 1972, a photoelectrochemical water-splitting titanium dioxide (TiO_2) electrode co-authored by Fujishima and Honda officially opened the door to semiconductor photocatalysis research [10]. Since then, it has been confirmed that various semiconductors are potential photocatalysts under ultraviolet or visible light, *e.g.*, graphite carbonitride (g-C_3N_4) [11], TiO_2 [12–14], bismuth vanadate ($BiVO_4$) [15], ZnO [16].

In order to improve the photocatalytic performance of semiconductors, a variety of strategies have been employed to improve the charge separation and transfer efficiency of photocatalysis, such as loading cocatalysts [17], introducing coating and supports [18] and fabricating semiconductor heterojunctions [19]. Among these methods, immobilizing the photocatalyst on the support can enhance the stability of the semiconductor, the adsorption capacity, the transfer efficiency, and the repeated utilization rate, which is an effective strategy to improve the photocatalytic performance [20]. One possibility to increase its photocatalytic activity is to introduce catalyst nanoparticles into the clay mineral structure [21]. Clay minerals are heterogeneous and lamellar structure materials with lots of advantages such as non-corrosive,

* Corresponding authors at: School of Water and Environment, Key Laboratory of Subsurface Hydrology and Ecological Effects in Arid Region of Ministry of Education, Chang'an University, Xi'an 710054, China.
E-mail addresses: wangqizhao@163.com, qzwang@chd.edu.cn (Q. Wang), h.cheng@cumtb.edu.cn (H. Cheng).

https://doi.org/10.1016/j.cclet.2021.01.009
1001-8417/

low-cost, environmentally friendly, abundant, high thermal stability, acid and alkali resistance [22–24]. In the case of clay supporting semiconductors, different clays have different mineralogical characteristics, which may result in different photocatalyst loading capabilities. Additionally, the natural reserves and mining conditions of clay minerals are different, which are directly related to the use cost of clay minerals, and can determine the application range of clay-photocatalyst composite materials [25]. Among the clay mineral, different from the tubular structure of halloysite and the rod-shaped structure of palygorskite, the layered structure of kaolinite can uniformly load semiconductors, increase reactive sites, and avoid the problem of easy agglomeration of semiconductors [26]. Kaolinite is very suitable for large-scale production and application of clay-photocatalyst composite materials due to its abundant natural reserves and mature mining technology. Furthermore, the hydroxyl (OH) groups between the kaolinite layers can participate in many chemical reactions and improve photocatalytic activity. Besides, kaolinite has been widely used as co-doping with semiconductors, since it not only has easy dispersibility, high adhesion, wide electrical insulation and good plasticity, but also has chemical properties such as acid and alkali resistance, high cations exchange capacity and excellent electron trapping ability [4]. In summary, kaolinite-based composite photocatalytic materials have excellent catalytic performance, low preparation cost and excellent chemical stability [27]. Therefore, it is worthy of further study on catalyst loading.

Herein, this paper presents a comprehensive overview on the recent advances in the design, synthesis, and applications of kaolinite-based photocatalysts. Firstly, the crystal structure and properties of kaolinite are introduced. Next, kaolinite-based photocatalysts (such as TiO_2/kaolinite, g-C_3N_4/kaolinite, g-C_3N_4/TiO_2/kaolinite, ZnO) are discussed in detail from the formation of heterostructures, synthesis-modification methods, photocatalytic mechanisms, and electron transfer pathways. Thirdly, this review presents photocatalytic applications of kaolinite-based photocatalysts in the fields of clean energy [28], pollutant degradation [29], and bacterial disinfection [30]. Finally, some concluding remarks and inspiring perspectives on future research of kaolinite-based photocatalysts for environmental purification and energy regeneration are presented.

2. Structure and properties of kaolinite

Kaolinite is a clay mineral with a chemical composition of $Si_2Al_2O_5(OH)_4$, the chemical composition is Al_2O_3 (39.50%), SiO_2 (46.54%) and H_2O (13.96%). The crystal is a layered silicate mineral of the triclinic system [31]. Generally, kaolinite is white color, sometimes the impurities contain red, blue or brown, and in the form of *pseudo*-hexagonal plates. Kaolinite has good plasticity and high adhesion, acid and alkali resistance, excellent electrical insulation, strong ion adsorption and weak cation exchange, as well as good sinterability and high fire resistance [32]. Due to the asymmetry of the interlayer space of kaolinite, hydrogen bonds are formed between adjacent layers, thereby obtaining strong cohesive energy. Based on the above factors, kaolinite is a multifunctional hydrated aluminosilicate with a wide range of application prospects, such as adsorption [33], discoloration [34], catalysis [35], photocatalysis [36], catalyst support [37] and modified catalyst [38].

Kaolinite belongs to aqueous aluminosilicate minerals consisting of the two-dimensional arrangement of Si-centered tetrahedra ($Si_2O_5^{2-}$) and Al-centered octahedra ($[Al_2(OH)_4]^{2+}$) (1:1 type mineral) [24]. The kaolinite crystal structure has local charge non-parallelism, the Si-centered tetrahedral layer carries more negative charges, and the Al-centered octahedral layer carries more positive charges [39]. The double-sided body layer is bonded by common oxygen atoms and the layered structure of kaolinite is tightly bonded together by hydrogen bonds (Fig. 1). The hydroxyl group (OH) existing between the kaolinite layers plays a vital role as the most active group and can participate in many chemical reactions [40].

Kaolinite is widely distributed in nature, mainly from aluminum-rich silicates under acidic conditions, weathered or low temperature hydrothermal replacement products [41]. The schematic drawing of the crystal structures of kaolinite nanoflakes as a combination of Si-centered tetrahedra with Al-centered octahedra is shown in Fig. 1. Additionally, there are a large number of active hydroxyl groups on the surface of kaolinite, which helps surface modification and makes kaolinite a suitable matrix for anchoring semiconductor particles to enhance photocatalytic activity [42].

Due to low cost, large specific surface area, high stability and adsorption capacity, traditional natural clay minerals have been widely used as carriers for photocatalytic materials [43]. The enhanced photocatalytic ability of clay-based photocatalysts is generally attributed to high adsorption performance and excellent surface properties to improve the dispersibility and specific surface area of semiconductors [44].

3. Kaolinite-based photocatalysts

A large number of studies show that kaolinite can exhibit great photocatalytic performance with very few semiconductors. The primary kaolinite-based photocatalytic materials comprise TiO_2/kaolinite [23,26,45–49], g-C_3N_4/kaolinite [6,28,50,51], g-C_3N_4/TiO_2/kaolinite [52,53], ZnO/kaolinite [30,54,55], ternary oxides/kaolinite [56,57] and other [58]. In this section, the synthesis methods and photocatalytic mechanism of materials and common measures to enhance photocatalytic activity are comprehensively summarized.

3.1. Kaolinite/TiO_2 composite

3.1.1. Properties of TiO_2

In recent decades, much research has been conducted on the development of nanoscale/structured TiO_2 as photocatalyst [59,60]. TiO_2 nanoparticles have a large surface area and various morphologies, which is beneficial for photocatalysis [61]. It is believed that nanoscale photocatalysts can demonstrate enhanced oxidation efficiency in photoreactors [62]. By summing up TiO_2 composite materials, the following two advantages are obtained: (a) The TiO_2 nanoparticles are fixed on the surface of a suitable particle matrix, and the particle size is micron order, which makes the operation using photocatalytic materials easier. (b) The composite material has a higher sedimentation tendency, which can effectively reduce the environmental impact caused by the release of nano-sized particles [63]. Anatase and rutile are two

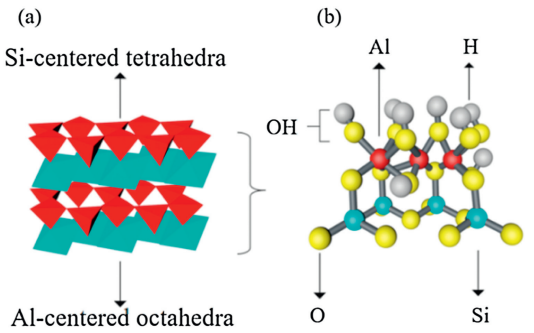

Fig. 1. The structure model of kaolinite (a) and the stick model of kaolinite (b).

main types of TiO_2 used for photocatalysis. Due to the differences in the crystal structure, crystal mass density, and electronic band structure, the anatase phase lattice contains more defects and dislocations, which can generate more oxygen vacancies to capture electrons. Photogenerated electrons and holes, therefore, are easier to separate and have strong photocatalytic activity. By contrast, rutile phase has weak adsorption capacity and small specific surface area, which caused that photo-generated electrons and holes are easy to recombine, and the catalytic activity is affected to some extent [64]. Additionally, it has been found that a mixture of anatase and rutile phase has a mixed crystal effect, which can effectively promote the generation of photo-generated electrons and the separation of hole charges in the anatase crystal and improve the photocatalytic activity [65].

3.1.2. Kaolinite/TiO_2 composite photocatalyst

The wide band of pristine TiO_2 is not suitable for visible light reception, which severely limits the practical application of TiO_2 [66]. In addition, the activity of TiO_2 is very limited even in the presence of co-catalysts, because the photocatalytic efficiency of TiO_2 is affected by the surface or internal electron-hole recombination process [67]. In order to overcome application limitations of TiO_2 in the field of photocatalysis, construction of binary photocatalytic systems is introduced as an ideal modification method. Here, we briefly outline the various manufacturing methods of kaolinite/TiO_2 composite materials, such as sol-gel method [23,40,46,47,68,69], hydrothermal method [70], wet impregnation [45], mechanical grinding method [71]. Among many synthesis methods, the sol-gel method, as a technology suitable for TiO_2 coating, has the following advantages: (a) Various types of supporting materials that cannot withstand high temperatures, such as rubber, wood or clay, can be used. (b) Liquid sol can be coated on base materials of various complex shapes. (c) It is easy to control the size of the crystal and obtain clear nanocrystals. (d) Low temperature synthesis can effectively maintain the internal structure of kaolinite and reduce energy consumption. In this regard, it was reported by Zhang *et al.* [29] the kaolinite/TiO_2 composites with mixed-phase TiO_2 was synthesized by a simple method at low temperature. The layer structure of kaolinite was destroyed to some extent, and a new double mesoporous structure was formed by embedding TiO_2 particles in the kaolinite layer. In other work, a 3D kaolinite foam carrier with an open-cell structure of alveolar polyurethane foam was produced by Pinato *et al.* [72] through shape memory synthesis, which greatly increased the exposed surface area of the TiO_2 photocatalyst film for light collection and liquid contact.

Modification of kaolinite with TiO_2 by hydrothermal method is also an effective method to improve the photocatalytic activity of composite materials. Hydrothermal method has the following advantages: (a) Nanomaterials synthesized by hydrothermal method have high purity and good grain development. (b) Avoid impurities and structural defects caused by post-treatment such as high temperature calcination or ball milling. (c) Hydrothermal methods generally do not negatively affect the performance of materials. In this regard, a previous study by Han *et al.* [73] stated that natural coal-containing kaolinite without thermal preactivation was combined with TiO_2 by a simple one-step hydrothermal method to improve its ability to catalyze fluoride removal. Immobilizing TiO_2 nanoparticles on the kaolinite aluminosilicate matrix can effectively reduce the environmental risk of TiO_2 nanoparticles and make the operation of this nanocomposite material safer. Furthermore, the nanocomposite kaolinite/TiO_2 was prepared by Kutlakova *et al.* [40] through thermal hydrolysis in the presence of kaolinite using titanium titanyl sulfate ($TiOSO_4$), and calcined kaolinite/TiO_2 at 600 °C. The high-temperature treatment effectively improved the photocatalytic activity of the composite. As we know, the photocatalytic performance of nanocomposites depends not only on the chemical composition, but also on the microstructure, size and morphology. Photocatalytic composite materials with uniform distribution and smaller particles usually have excellent stability, stronger surface adsorption, and higher loading efficiency.

The mechanical mixing method is a pure physical process of powder particle surface modification method, which can effectively combine kaolinite with nano-TiO_2, and has the following advantages: (a) The experimental equipment of the mechanical mixing method is simple and easy to operate. (b) The mechanical mixing method has little effect on the material properties. (c) Low energy consumption and safe operation. However, mechanical mixing cannot be used in all situations. The mixing of a small amount of insoluble powdered solids and liquids, but stirring can not change the particle size of the powdered solids. If the solid particles cannot make the sedimentation speed less than the flow speed of the liquid before mixing, a uniform suspension will not be formed regardless of the stirring method. In addition, mechanical mixing usually takes a long time, increasing the time cost. In this aspect, it was demonstrated that interfacial chemical bonds can effectively regulate the photogenerated charge transfer in nanoclay-based heterostructures composed of natural kaolinite nanosheets and TiO_2 [71].

Kaolinite/TiO_2 photocatalytic materials obtained by different synthesis methods have different properties primarily in morphology, structure, surface character, and photocatalytic performance.

The structure of kaolinite/TiO_2 composites are mostly laminar loaded with nanoparticles and porous laminar. Some scholars use the intercalation method to change the structure of kaolinite to prepare cylindrical rod-shaped and curved layered composite materials to increase the specific surface area of the photocatalyst. A binary mixture of anatase and rutile or brookite existed in the kaolinite/TiO_2 composite synthesized by Zhang *et al.* [29] with increasing synthesis temperature. Transmission electron microscope (TEM) analysis has shown two interconnected crystal phases of TiO_2, indicating the anatase–brookite and anatase–rutile nanocrystal heterojunctions are formed in the sample. Furthermore, the polyurethane sponge 3D kaolinite foam material prepared by Pinato *et al.* [72] has an alveolar open cell structure. The alveolar open cell is a repeating unit of a dodecahedron, and each unit is composed of 12 pentagons. The particle size of TiO_2 nanoparticles largely depends on the morphology of the support. At the same time, the particle size of the exposed TiO_2 is significantly larger than that of the TiO_2 nanoparticles supported on kaolinite, indicating that kaolinite has a good dispersion effect on TiO_2 clusters. Moreover, Han *et al.* [73] confirmed the formation of anatase nanoparticles (<10 nm) on the surface of kaolinite. TEM images of kaolinite/TiO_2 composites synthesized by Jiang *et al.* [71] showed that the TiO_2 nanoparticles overlaid on kaolinite had a *pseudo*-hexagonal platelet structure.

The surface properties of kaolinite/TiO_2 photocatalytic materials are usually related to their modification methods. The sol-gel method can uniformly load the precursors on the surface of the kaolinite layer, while calcination technique can effectively improve the pore structure of the composite material and increase the reactive sites. In addition, the intercalation treatment of kaolinite can bend the layered structure of kaolinite and significantly increase the specific surface area of the material. The kaolinite/TiO_2 composites synthesized by Zhang *et al.* [29] form a new porous structure with specific surface area ranging from 61.35 m^2/g to 113.5 m^2/g, which is much larger than that of kaolinite (27.45 m^2/g). The average pore size of the composite material is 9.606 nm. The large specific surface area of kaolinite/TiO_2 composites can provide more adsorption and photocatalytic active

sites for the degradation of organic molecules. Similarly, The specific surface area and the average pore size of high-performance TiO_2 coated alveolar kaolinite foam photocatalyst prepared by Pinato *et al.* [72] are 209.4 m^2/g and 5.86 nm, respectively. Through the dialysis process, the soluble ions can be removed uniformly and slowly to increase the pH of the sol. Therefore, agglomerates will slowly form in the sol, resulting in higher porosity and specific surface area. Furthermore, the nanocomposite synthesized by Han *et al.* [73] retains the kaolinite crystal structure, but the specific surface area reaches 118.0 m^2/g.

The photocatalytic performance tests of kaolinite/TiO_2 materials mostly focus on the degradation of organic dyes, volatile organic gases, reduction of heavy metals, and bacterial inhibition. Compared with pure TiO_2, the catalytic performance of the composite catalyst has been significantly improved. The composites synthesized by Zhang *et al.* [29] showed excellent photocatalytic activity for the degradation of 4-nitrophenol. The new larger mesopores formed by TiO_2 particles embedded in kaolinite made the reactive molecules easily diffuse in the reaction, which was beneficial to the photocatalytic reaction. High-efficiency photocatalysts made by shape memory synthesis at low temperatures could also increase the exposed surface area and increase the amount of light collected. For instance, the TiO_2 coated alveolar clay foam photocatalyst [72] had the best photocatalytic performance in an acidic environment with a pH of 2. The excellent photocatalytic performance was attributed to the larger surface area for both light harvesting and liquid contact area. The removal rate of cumene hydroperoxide (CHP) by the photocatalyst was 94%, and the CHP removal rate of 94%–96% was still retained through the four-cycle recycling test. It was proposed that two main factors affecting the photocatalytic activity of the complex are surface adsorption and light-induced charge transfer. Moreover, as the content of TiO_2 in the nanocomposite [73] increased from 0% to 50% by mass, the removal efficiency of fluorine increased from 15% to 87%, which indicated that the defluorination ability of kaolinite modified with TiO_2 had been significantly improved. The adsorption kinetics of fluoride was in good agreement with the *pseudo*-second-order kinetic model, and nanocomposites had extremely strong adsorption capabilities. In another report, compared with commercial TiO_2 nanoparticles (P25), kaolinite/TiO_2 [71] showed significantly improved photocatalytic ability, the rate of photodegradation of methyl orange (MO) in composites was 2.5 times that of pure P25. The adjustment of interface chemical bonds improved the separation and transfer efficiency of photogenerated charges, and enhances the photocatalytic activity. Interface engineering that regulated interface charge transfer through chemical bonds was an effective method for synthesizing highly efficient heterostructure photocatalysts.

In summary, the sol-gel method can effectively inhibit the oxidation process of the product by performing the reaction in an organic solvent. Under the same conditions, the solvothermal can reach a higher gas pressure than hydrothermal synthesis, which is beneficial to the synthesis of the product. At lower temperatures, the structural units in the reactants can remain in the product without being destroyed. However, hydrothermal and sol-gel methods also have some problems, for example, the process of material synthesis cannot be observed. The equipment requires high temperature and high-pressure steel, corrosion-resistant lining, technical difficulty, strict temperature and pressure control, and high cost. When heated and sealed, the reaction kettle generates a great pressure, which poses a big potential safety hazard. From the performance of photocatalyst the mixture of TiO_2 and natural kaolinite can form a nanocomposite material with good catalytic performance. The photocatalytic activity is directly related to the presence of silanol and aluminum alcohol groups of kaolinite, which has excellent adsorption capacity. Kaolinite-based photocatalysts usually have a higher specific surface area and convenient porosity to effectively enhance photocatalytic activity. Moreover, better dispersion and smaller particle size of nano-TiO_2 on the surface of kaolinite, and strong electrostatic repulsion also play a key role in the enhancement mechanism.

3.1.3. Photocatalytic mechanism of kaolinite/TiO_2 composite

The photocatalytic mechanism of kaolinite/TiO_2 nanocomposites may be due to the synergy between kaolinite and supported TiO_2 nanoparticles [74]. The essence of TiO_2 photocatalysis is the electron transporter that acts as a redox reaction [75]. The photocatalytic mechanism of kaolinite/TiO_2 nanocomposite mainly includes the following two types: Superoxide radical degradation mechanism and hydroxyl radical degradation mechanism.

When TiO_2 supported on kaolinite absorbs photons, the valence band electrons are excited to the empty conduction band, forming a negatively charged electron e^-, and the valence band generates a positively charged hole h^+ (Fig. 2). Photogenerated holes have the strong electron-reducing ability and strong oxidation. These photoelectron holes react with oxygen molecules (O_2), H_2O, or hydroxyl groups on the surface of kaolinite to form hydroxyl radicals ($^{\bullet}OH$) and superoxide radical anions ($O_2^{\bullet-}$). $^{\bullet}OH$ has strong oxidation properties [76]. The complete equations of mechanism reactions are as follows (Eqs. 1–13):

$$TiO_2 + h\nu \rightarrow TiO_2(e^- + h^+) \quad (1)$$

Reaction involving valence band h^+

$$TiO_2(h^+) + H_2O \rightarrow TiO_2 + {}^{\bullet}OH + H^+ \quad (2)$$

$$TiO_2(h^+) + OH^- \rightarrow TiO_2 + {}^{\bullet}OH \quad (3)$$

$$TiO_2(h^+) + 2H_2O \rightarrow TiO_2 + H_2O_2 + 2H^+ \quad (4)$$

Reaction involving conduction band e^-

$$TiO_2(e^-) + O_2 \rightarrow TiO_2 + O_2^{\bullet-} \quad (5)$$

$$O_2^{\bullet-} + H^+ \rightarrow HO_2^{\bullet} \quad (6)$$

$$TiO_2(e^-) + HO_2^{\bullet} \rightarrow TiO_2 + HO_2^- \quad (7)$$

$$TiO_2(e^-) + HO_2^{\bullet} + 2H^+ \rightarrow TiO_2 + H_2O_2 \quad (8)$$

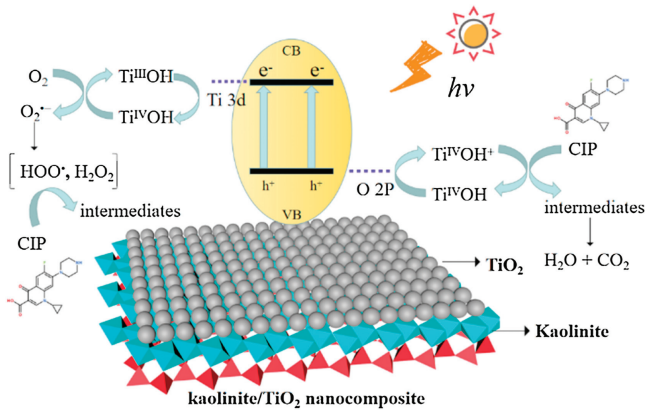

Fig. 2. Schematic illustration of photocatalytic reaction mechanism of kaolinite/TiO_2 nanocomposites.

$$TiO_2(e^-) + H_2O_2 \rightarrow TiO_2 + OH^- + {}^{\bullet}OH \quad (9)$$

$$O_2^{\bullet-} + H_2O_2 \rightarrow OH^- + {}^{\bullet}OH + O_2 \quad (10)$$

$$2HO_2^{\bullet} \rightarrow O_2 + H_2O_2 \quad (11)$$

$$R-H(C*molecules) + {}^{\bullet}OH \rightarrow R^{\bullet} + H_2O \quad (12)$$

$$R-H(C*molecules) + H^+ \rightarrow R^{+\bullet} \rightarrow Degredation \quad (13)$$

3.2. Kaolinite/g-C_3N_4 composite

3.2.1. Properties of g-C_3N_4

g-C_3N_4 is a typical polymer semiconductor. The CN atoms in the structure hybridize with sp^2 to form a highly delocalized π conjugated system. It is considered to be the most stable allotrope of various carbon nitrides under natural environmental conditions [77]. In recent years, g-C_3N_4 has attracted more and more attention due to the suitable bandgap, easy preparation, good chemical tenability, superior visible-light response, environmentally friendly superiority and low-cost [78]. Wang and his coworkers firstly discovered the photocatalytic water splitting evolution over g-C_3N_4 in 2009 [79]. Since g-C_3N_4 has a similar layered structure to graphite, the theoretical specific surface area of an ideal monolayer may be as high as 2500 m^2/g [80]. Furthermore, the polymerization properties of g-C_3N_4 make the structure flexible enough and have a matrix that has excellent compatibility with various inorganic nanoparticles, and can control surface chemistry through molecular-level modification and surface engineering to produce excellent g-C_3N_4 composite materials. Therefore, due to the unique characteristics of g-C_3N_4, it can be widely used as a photocatalyst in various environments [81].

Thermal polymerization is considered to be the most common method for synthesizing g-C_3N_4 because it is easy to handle, low cost, better available raw materials and better crystalline forms [82]. g-C_3N_4 can be easily prepared by thermally condensing several low-cost nitrogen-rich precursors, such as cyanamide [83], melamine [84], dicyandiamide [85], thiourea [86], Urea [87], or mixtures thereof.

3.2.2. Kaolinite/g-C_3N_4 composite photocatalyst

Although some modification methods can partially improve the defects of g-C_3N_4, it is still difficult to avoid the disadvantages of easy aggregation, low adsorption capacity, difficult separation and high cost [88]. It was proven that the introduction of natural minerals could not only improve the photocatalytic efficiency, but also maintain the photocatalytic activity of the catalyst, facilitate separation and recycling, and promote the rapid adsorption of pollutants on the surface of composite photocatalysts [89]. Combining with the unique crystal structure of kaolinite, several of kaolinite heterojunctions based on g-C_3N_4 were synthesized. Here, we briefly outlined various synthetic methods of kaolinite/g-C_3N_4 composite materials, such as mechanochemical treatment [90], thermal polymerization [6,28,50,51,91], self-assembly [4]. Among many synthetic methods, mechanochemical treatment technology combines the advantages of chemical grinding and mechanical grinding, and has some outstanding advantages for the synthesis of photocatalytic materials: (a) Mechanochemical treatment has low damage to materials, good integrity, and is not prone to surface/subsurface damage. (b) Material removal efficiency can be guaranteed. (c) Mechanochemical treatment can obtain a more perfect surface, and the resulting flatness is 1–2 orders of magnitude higher than that of the two kinds of grinding alone, and it can achieve nano-to-atomic surface roughness. For instance, a kaolinite/g-C_3N_4 composite with enhanced visible-light-driven photocatalytic activity was prepared through a simple mechanochemical method [90]. g-C_3N_4 and kaolinite can be closely combined by mechanical grinding to produce a synergistic effect, generating more adsorption and photocatalytic reaction sites, effectively reducing the probability of recombining photo-generated electron-hole pairs.

Thermal polymerization is one of the methods for manufacturing polymers. It is a chain polymerization reaction in which the thermal energy of the monomer molecule is initiated and activated into a free radical. Thermal polymerization has the following advantages: (a) The product has less impurities and high purity. (b) The production equipment has high utilization rate and simple operation, and does not require complicated separation and purification operations. (c) The thermal polymerization production process is simple, the process is short and easy to be continuous, and the production cost is low. In this regard, many studies have synthesized kaolinite/g-C_3N_4 composite photocatalyst by thermal polymerization and some modification methods. For instance, the insertion of certain polar organics into the kaolinite intermediate layer can open the asymmetric intermediate layer space and create a two-dimensional limited microenvironment for the insertion reaction [92]. Kaolinite intercalation composites have both the unique adsorption and dispersion properties of clay minerals and the reactivity of organic compounds. Intercalation reactions are one of the effective methods for synthesizing photocatalytic composite materials. Furthermore, acid-modified polymers can effectively increase the efficiency of charge transfer in photocatalytic reactions [93]. Cyanuric acid as a modifier was used by Sun [6] *et al.* to synthesize a new cyanuric-acid-modified graphitic carbon nitride composite (m-g-C_3N_4/kaolinite) material in a two-step process.

Self-assembly means that molecules or nanoparticles spontaneously organize or aggregate into a stable structure with a certain geometric appearance under the interaction based on non-covalent bonds. The synthesis of photocatalytic materials through self-assembly has the following advantages: (a) The self-assembly technology is simple and easy to use, and no special device is needed. (b) Self-assembly usually uses water as a solvent, which has the advantages of deposition process and molecular control of membrane structure. (c) Self-assembly can use the continuous deposition of different components to prepare a two-dimensional or even three-dimensional ordered structure between the film layers to achieve the optical, electrical, and magnetic functions of the film. In this regard, Dong and co-workers [4] uniformly peeled the stacked g-C_3N_4 and bismuth oxychloride (BiOCl) into ultra-thin nanosheets, and used the interlayer self-assembly to fix the nanosheets on the kaolinite flakes one by one, and built a new BiOCl/g-C_3N_4 with a "sandwich" structure.

The properties of kaolinite/g-C_3N_4 nanocomposite photocatalytic materials are summarized as follows: g-C_3N_4 has a layered structure similar to kaolinite and can be combined with kaolinite to form a sandwich structure. For example, the kaolinite/g-C_3N_4 composite material prepared by Sun *et al.* [90] has a relatively rough two-dimensional sheet structure, and the kaolinite layer is densely and uniformly decorated with g-C_3N_4 nanosheets. The layered structure of natural kaolinite can provide sufficient surface area, not only can adsorb pollutants, but also can be in close contact with the g-C_3N_4 nanosheets in the composite material. Similarly, from the XRD patterns of g-C_3N_4/kaolinite and m-g-C_3N_4/kaolinite composites [6], it is clear that they show only one peak at 27.67° (002), which indicates that g-C_3N_4 has been successfully loaded

onto the surface of kaolinite. Scanning electron microscopy shows that kaolinite is composed of many parallel nanosheets, which is a typical two-dimensional layered structure. It is very tightly combined with the g-C_3N_4 nanosheets in the composite material, which can provide a large surface area to enhance the ability to adsorb pollutants. Moreover, compared with g-C_3N_4/kaolinite composites, the surface of acid-modified g-C_3N_4/kaolinite becomes more porous and uniform, which is considered to be the reason for the volatilization of cyanuric acid in the precursor during the calcination of the composite. In short, the introduction of cyanuric acid effectively improved the pore structure of g-C_3N_4 in the binary system and provided more active sites for photodegradation of pollutants. Furthermore, as shown in the SEM picture, nano-flaky kaolinite with clear edges and smooth surface, g-C_3N_4 with irregularly wrinkled flake form and BiOCl with smooth and flat form were successfully peeled into flakes, and g-C_3N_4 and BiOCl ultra-thin nanosheets are evenly distributed on the surface of kaolinite layer with "sandwich" structure, which proves the structure of BiOCl/g-C_3N_4/kaolinite ternary heterostructure [4].

The g-C_3N_4/kaolinite composite material usually has a large specific surface area due to its sandwich structure. The acid treatment and gas stripping treatment of the composite material can produce a porous sandwich structure, which further increases the specific surface area and pore volume. Compared with kaolinite and g-C_3N_4, the specific surface area and pore volume of g-C_3N_4/kaolinite composite increased significantly to reach 31.72 m^2/g and 0.07 cm^3/g, respectively [90]. The results show that the synergistic effect of kaolinite with unique structure and g-C_3N_4 is beneficial to increase the specific surface area of the composite material, improve the adsorption capacity of pollutants, and provide more surface active sites for the degradation of pollutants. Moreover, the specific surface area of m-g-C_3N_4/kaolinite composite material synthesized by Sun *et al.* [6] is 49.522 m^2/g, and the pore volume is 0.088 cm^3/g. It is found that large surface area and total pore volume can effectively enhance the adsorption and photocatalytic capabilities [94]. The calculated band gap of CN is 2.72 eV, and all band gaps of m-g-C_3N_4/kaolinite composites are 2.72 ± 0.01 eV, indicating that the introduction of cyanuric acid has little effect on the bandgap of g-C_3N_4. The cyanuric acid-modified g-C_3N_4/kaolinite composite has rich pore structure and reaction sites. Furthermore, the pore volume and average pore radius of BiOCl/g-C_3N_4/kaolinite composites synthesized by Dong *et al.* [4] are larger than those of bulk BiOCl, reaching 0.088 cm^3/g and 10.914 nm, respectively, and the specific surface area is increased by 50% compared to kaolinite, reaching 32.088 m^2/g. Which is caused by the formation of ultra-thin BiOCl nanosheets and g-C_3N_4 nanosheets and a unique "sandwich" structure, the adsorption and absorption capabilities of the composite material are enhanced.

The photocatalytic performance test of kaolinite/g-C_3N_4 material mainly focused on the degradation of organic dyes, water splitting and hydrogen evolution. The photocatalytic composite material synthesized after mechanochemical treatment showed excellent photocatalytic activity, and had good photocatalytic degradation activity of Rhodamine B (RhB) under visible light irradiation, and its reaction rate constant was almost 4.0 times that of pure g-C_3N_4 [90]. The enhanced photocatalytic activity of kaolinite/g-C_3N_4 composite was attributed to the synergy between g-C_3N_4 and kaolinite, which enhanced the adsorption capacity, increased the specific surface area, extended the life of photogenerated carriers, and effectively suppressed photogenerated electron-hole pair recombination. Moreover, the removal rate of RhB of the m-g-C_3N_4/kaolinite composite material after visible light irradiation for 180 min was as high as 93%, which was about 2 times and 9 times higher than bare g-C_3N_4 and standard P25, respectively [6]. During thermal polymerization, cyanuric acid decomposed at about 330 °C and generated a large number of pore structures and reaction sites in the composite, which greatly increased the specific surface area of the composite, improved the adsorption capacity and further enhanced the photocatalytic performance. Furthermore, the BiOCl/g-C_3N_4/kaolinite composite material showed excellent photocatalytic performance in the photodegradation of formaldehyde and organic matter [4]. The formaldehyde removal rate was as high as 74.55%. After 120 min of exposure, the composite material's degradation efficiency of RhB reached 97%. The enhanced photocatalytic performance of nanosheet composites may be attributed to the close contact formed between the interfaces, which resulted in higher charge separation efficiency and stronger pollutant adsorption capacity. Besides, experimentally obtained reactive oxidizing substances (especially h^+) played a vital role in photocatalytic reactions.

Based on the above overview, the thermal polymerization method forms a kaolinite/g-C_3N_4 composite material by thermally inducing the polycondensation reaction of the precursor, which is a direct and simple method for preparing the material. It has the advantages of low cost, low equipment and control requirements, simple operation, easy enlargement, and many types of precursors. However, the synthesis of g-C_3N_4 is a complex thermochemical reaction process. Different degrees of polycondensate can coexist in a wide temperature range. It is difficult to prepare carbon nitride polymers that contain only a single molecular structure. When the temperature reaches 700 °C, the material begins to decompose violently, generating gases such as NH_3 and $C_xN_yH_z$ [95]. Therefore, controlling the synthesis temperature is a key factor in preparing composite materials. In terms of the performance of composite photocatalytic materials, the combination of nano-g-C_3N_4 and kaolinite with unique structure can produce excellent photocatalytic activity, kaolinite/g-C_3N_4 composite usually has a larger specific surface area, and improved electron transport ability and fast charge separation efficiency. The interface between g-C_3N_4 and kaolinite is tightly combined, resulting in a rich pore structure and reaction sites to effectively separate the photogenerated electron-holes, thereby improving the activity of the composite photocatalyst.

3.2.3. Photocatalytic mechanism of kaolinite/g-C_3N_4 composite

Based on the above literature summary, the possible photocatalytic mechanism and potential electron transfer pathway of kaolinite/g-C_3N_4 nanocomposites are as follows: Under visible-light irradiation, the electrons (e^-) in valence band (VB) of g-C_3N_4 were excited to conduction band (CB), while the corresponding holes (h^+) remained in the VB (Fig. 3) [96]. As we all know, there is

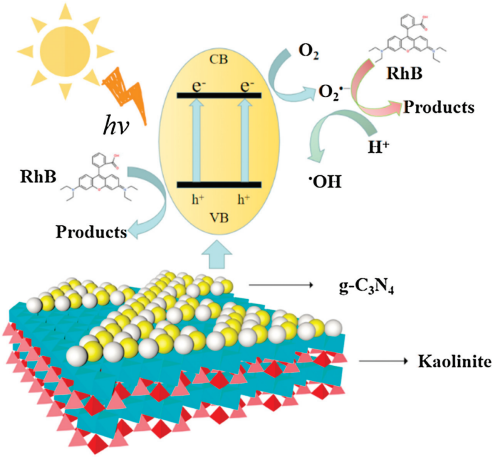

Fig. 3. Schematic illustration of the charge separation and photocatalytic mechanism of kaolinite/g-C_3N_4 composites under visible light irradiation.

electrostatic repulsion between the same electrical electrons, and electrostatic attraction between different electrical electrons. The layered surface of kaolinite usually has a negative charge [97], which accelerates the migration rate of excited e^- and the e^- on CB can combine with the oxygen absorbed on the surface of the composite to produce superoxide ($O_2^{\bullet-}$). Then, $O_2^{\bullet-}$ reacts with water molecules to generate hydroxyl radicals ($^{\bullet}OH$), OH^- and O_2, and the product $^{\bullet}OH$ can also react with the target [98].

3.3. Kaolinite/TiO_2/g-C_3N_4 composite

3.3.1. TiO_2/g-C_3N_4 heterojunction

Conventional semiconductor photocatalysts (such as TiO_2 and g-C_3N_4) usually have poor activity, narrow spectral response and limited electron transmission, poor reusability, and inconvenient recycling, which have a huge impact on the practical application of photocatalyst [99]. It was found that two photoreactive semiconductors with suitable electronic structures by constructing heterojunctions (such as g-C_3N_4/TiO_2) have excellent photocatalytic activity. The traditional type II heterojunction based on g-C_3N_4 can be constructed by g-C_3N_4 and another semiconductor, where the CB and VB positions of one semiconductor are higher or lower than the other semiconductor. The difference in chemical potential between the two semiconductor units causes the band bending at the contact interface of the heterojunction. Band bending can form internal electric field. The internal electric field in the heterojunction accelerates the separation of photogenerated electrons and holes, which is the main driving force for enhanced photocatalytic performance. In particular, when the photon energy is higher than or equal to the band gap of two semiconductors, the two cells of the heterojunction can be excited at the same time. On the other hand, when photon energy can only excite one unit, another semiconductor can act as an electron/hole acceptor. In both cases, the separation efficiency of electron-hole pairs can be improved [100]. Heterojunction photocatalysts with different morphologies and structures also have different physical and chemical properties. Hollow core-shell nanospheres will provide abundant specific surface area. A Ti^{3+} self-doped TiO_2/g-C_3N_4 hollow core-shell nano-heterojunction was synthesized through continuous hydrothermal deposition and sculpture reduction processes [101]. The TiO_2/g-C_3N_4 nano-heterojunction exhibited superior photocatalytic activity 18 times and 65 times stronger than that of ordinary TiO_2 and g-C_3N_4, respectively. The large contact surface area between the two semiconductors facilitates effective spatial redistribution of charges at the heterojunction interface. This redistribution of charges can effectively promote the separation of charges and enhance photocatalytic performance.

3.3.2. TiO_2/g-C_3N_4/kaolinite composite photocatalyst

Generally, most of the current research on kaolinite-based photocatalytic composites has focused on the traditional type II heterojunction, the traditional type II heterojunction can effectively perform space charge separation to a certain extent, however, the type II heterojunction has weaker photo-electron and hole redox capabilities because the VB and CB of the heterojunction semiconductor carry less positive and negative charges. In this case, it is difficult for a pair of semiconductors with a narrow band gap to achieve both excellent charge separation efficiency and excellent redox ability at the same time. Fortunately, the Z scheme heterojunction can effectively solve this problem. For the Z scheme heterojunction, the light-induced electron transfer of the semiconductor II with a negative CB value is transferred to the semiconductor I with a VB value through the contact interface, and is further excited to the CB of the semiconductor I, leaving a hole in the VB of the semiconductor II (Fig. 4). By retaining the high negative CB edge and high positive VB edge, the Z-type

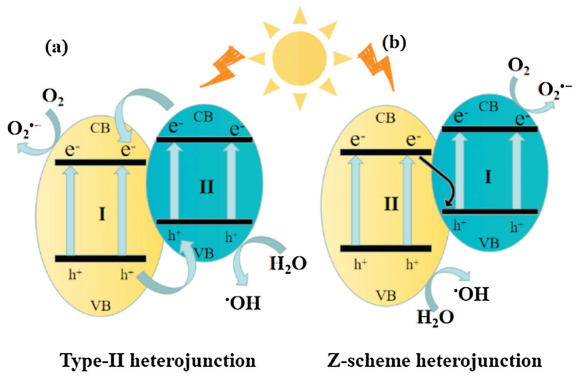

Fig. 4. Traditional type-II heterojunction (a) and direct Z-scheme heterojunction (b).

heterojunction can use semiconductor pairs with a narrow band gap without losing photogenerated electrons and strong redox capabilities [102]. Nowadays, there are many synthesis methods for kaolinite-based heterojunctions of TiO_2/g-C_3N_4. Kaolinite-based heterogeneous photocatalysts have good dispersibility and enhanced visible light absorption capacity. For example, Li *et al.* [52] used chemical stripping and automatic assembly to prepare a 3D heterogeneous g-C_3N_4/TiO_2/kaolinite composite with enhanced photocatalytic activity through a mild sol-gel method. The g-C_3N_4/TiO_2/kaolinite composite was observed from the SEM image, and a 3D "sandwich" structure was successfully established through the hydrogen ion functionalization process. The composite material has a tight binding and highly exposed edges, which is conducive to increasing the number of active sites and improving the ability of the carrier to transfer and migrate [103]. The g-C_3N_4/TiO_2/kaolinite composite has a relatively porous structure, which further increases the light-trapping ability [104]. After loading kaolinite, the grain size of TiO_2 decreased significantly from about 30 nm to 14 nm. The introduction of kaolinite can effectively reduce the grain size of the supported TiO_2 nanoparticles, which is conducive to the enhancement of photocatalytic activity. In addition, compared with g-C_3N_4, the absorptive capacity of the hetero composite material is significantly enhanced in the visible light region of 450–800 nm. The constructed "sandwich" structure can improve the utilization efficiency of visible light and facilitate the photocatalytic reaction. The specific surface area and total pore volume of g-C_3N_4/TiO_2/kaolinite composite materials reached 51.596 m^2/g and 0.100 cm^3/g, which are significantly higher than any single material. The improvement in photocatalytic performance should be attributed to enhanced visible light absorption capacity and the Z-scheme transport of photogenerated electrons.

3.3.3. Photocatalytic mechanism of TiO_2/g-C_3N_4/kaolinite composite

Generally, the performance of a photocatalyst depends on two key characteristics, (a) the ability to utilize the solar spectrum and (b) the efficiency of the generated electron-hole pairs to generate reactive oxygen species [105]. Based on the above literature analysis, the possible Z scheme mechanism is proposed as follows: Under visible light irradiation, electrons are excited, and photoinduced holes in TiO_2 remain in VB, while electrons will be transferred from the conductive band CB of TiO_2 to the VB of g-C_3N_4. The electrons in the VB of g-C_3N_4 then tend to transition to its CB. The holes of TiO_2 in VB and the electrons of g-C_3N_4 in CB will be effectively separated (Fig. 5) [106]. Moreover, negatively charged kaolinite can generate strong electrostatic repulsion, which is beneficial for the separation of photo-generated carriers [107]. The hydroxyl groups rich in kaolinite surface form new Ti—O—H bonds during the preparation process, which improves

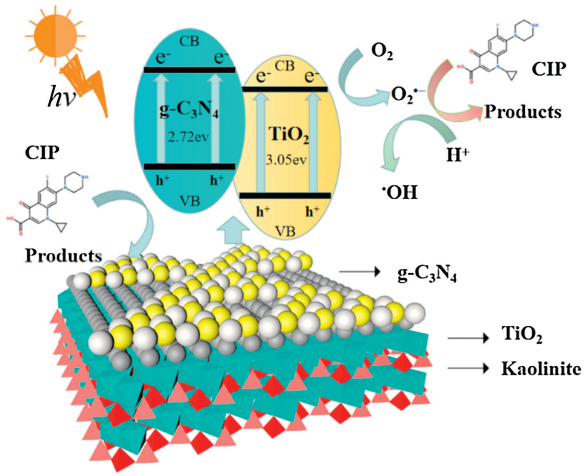

Fig. 5. Z-scheme g-C_3N_4/TiO_2/Kaolinite composite material degradation process mechanism scheme.

the efficiency of separating the carrier [108]. The electrons in the CB position of g-C_3N_4 will reduce O_2 to $O_2^{\bullet-}$. In addition, the absorbed O_2 can also react with water molecules and electrons to form hydrogen peroxide. Finally, some of the generated H_2O_2 and $O_2^{\bullet-}$ can be converted into hydroxyl ($^{\bullet}OH$) [109]. The main active specie ($O_2^{\bullet-}$) and the subordinate species ($^{\bullet}OH$ and h^+) could effectively degrade contaminants.

3.4. Kaolinite/ZnO composite

Zinc oxide crystals (ZnO) have three structures: hexagonal wurtzite structure, cubic sphalerite structure, and rock salt octahedral structure [110]. Besides, pure zinc oxide is colorless and transparent. ZnO is an n-type semiconductor. At room temperature, the energy band gap of zinc oxide is about 3.3 eV, and the electrons in the valence band can accept the energy in the ultraviolet light to undergo transition and generate hydroxyl radicals [30]. Nowadays, ZnO is the most widely studied low-cost semiconductor material, due to its good photocatalysis, piezoelectricity, antibacterial properties, significant light corrosion resistance and excellent free excitation binding energy. However, the toxicity of ZnO and its potential risks to the environment and human health are still a major problem that limit its application [111]. In order to reduce the environmental risk of ZnO, ZnO can be anchored on a suitable solid substrate, which can not only restrict the movement of ZnO nanoparticles, but also can still exert its unique photocatalytic performance.

Many scholars choose kaolinite as the carrier of ZnO because of its safety, pollution-free, cheap, and unique layered structure. ZnO/Kaolinite composite can be prepared *via* various methods (hydrothermal method, electrochemical growth, chemical vapor deposition, sol-gel method). The structure of composite materials are mostly flocs, rod-shaped, and flakes with particles. For example, the kaolinite/ZnO nanocomposite with a variety of ZnO nanoparticles was prepared by a simple hydrothermal method [54]. On the one hand, the calcination of nanocomposites at 600 °C leads to a phase transition of kaolinite, and ZnO crystals further grow on the surface of metakaolinite. On the other hand, composite materials have excellent photocatalytic activity. After 1 h of ultraviolet irradiation, the degradation rate of ZnO/kaolinite nanocomposite to Acid Orange 7 aqueous solution reached 95%. Furthermore, ZnO/kaolinite was synthesized by co-precipitation technology [30], and it was found that ZnO/kaolinite is more effective than Fe-doped ZnO and TiO_2 in the photocatalytic disinfection process. Under 120 min of visible light irradiation, *Escherichia coli* was completely degraded. Moreover, kaolinite can be made into thin sheets by simple peeling, and then dealuminated into nano-rolls by ultrasonic radiation and organic expansion. Compared with primitive kaolinite, kaolinite nanotubes have a high specific surface area, high adsorption capacity and a good ordered porous structure [55]. In this case, kaolinite nanotubes were synthesized through a simple rolling process, and a new type of nanocomposite material (ZnO/kaolinite nanotubes) was synthesized by the sol-gel method [112]. In the presence of visible light source, it has high catalytic activity for the oxidation of levofloxacin. After 75 min, 30 mg/L of levofloxacin was completely oxidized.

All studies show that ZnO/kaolinite composite can effectively prevent the migration of ZnO, reduce the environmental risk, and increase the reactive sites to a certain extent, and strengthen the photocatalytic activity.

3.5. Kaolinite/ternary oxides composite and other

More recently, Ternary oxides (such as bismuth oxyhalide, ferrites, tungstate and vanadate) have attracted special attention in the field of photocatalysis due to their unique physical and chemical properties and potential photocatalytic properties [8,113,114].

Currently, the crystalline $CuFe_2O_4$ nanoparticles with spinel structure are a potential peroxymonosulfate catalyst due to its high catalytic activity and low metal ion leaching characteristics. However, $CuFe_2O_4$ nanoparticles are easy to agglomerate, which greatly reduces the specific surface area of reactive sites [115]. The two-dimensional layered structure of kaolinite is a suitable platform for the grafting of $CuFe_2O_4$ nanoparticles. In addition, a large number of aluminum hydroxyl groups and permanent negative charges on the surface of kaolinite effectively prevent the self-aggregation of $CuFe_2O_4$ nanoparticles by adjusting the crystallization. Taking into account of these factors, the $CuFe_2O_4$/kaolinite photocatalyst is prepared by a simple citrate combustion method [57]. The photocatalytic activity was evaluated by activating peroxide monosulfate to destroy bisphenol A. Compared with bare $CuFe_2O_4$, 40%-$CuFe_2O_4$/kaolinite has a larger specific surface area, larger pore volume, more hydroxyl groups and more accessible reaction sites, and the reaction rate constant is about 5.5 times that of bare $CuFe_2O_4$. Furthermore, the discrete $CuFe_2O_4$ nanoparticles are uniformly anchored on the surface of the kaolinite through Fe-O-Al bonds, effectively preventing the leaching of metal ions and increasing the stability of the composite material.

Compared with montmorillonite and palygorskite, kaolinite has a low cation exchange capacity, and a small specific surface area leads to a lower adsorption capacity [56]. Incorporating inorganic particles such as spinel ferrite into the kaolinite matrix can improve its adsorption capacity. The kaolinite/$CoFe_2O_4$ nanoparticle composite synthesized by Olusegun *et al.* [116]. Exhibits excellent adsorption performance for doxycycline and Congo red.

Silver halide is highly sensitive to light, has appropriate and effective photoactivity, and is used as a photosensitizer [117]. However, continuous reduction of silver (Ag^+) ions in the moving gap to silver (Ag^0) atoms will cause photo-corrosion on the semiconductor surface, which limits its practical application. In this case, Tun *et al.* [58] synthesizes a new type of visible light-responsive Ag@AgBr/kaolinite photocatalyst by *in-situ* precipitation-precipitation method. The synthesized Ag@AgBr/kaolinite photocatalyst has excellent visible light catalytic activity for the degradation of methyl orange. The catalyst exhibits effective photocatalytic activity in a wide pH range of 2.54–10.95. In addition, the photo-induced holes (+2.74 eV) in the AgBr valence band participate in the H_2O/OH^- oxidation reaction. The valence

band is higher than $^{\bullet}OH$ (1.99 eV *vs.* SHE). The formed $^{\bullet}OH$ radicals are strong oxidants that directly degrade organic dyes. Similarly, a novel Ag/g-C_3N_4/kaolinite composite photocatalyst was fabricated by Sun *et al.* [118] through employing *in situ* calcination and a photodeposition process. The synthesized Ag/g-C_3N_4/kaolin composite has a higher degradation rate of ibuprofen, and the reaction rate under visible light irradiation is 1.87 times that of the Ag/g-C_3N_4 composite. The prepared composite material has a higher specific surface area (35.96 m^2/g) and pore volume (0.080 cm^3/g). The photogenerated electrons in the reaction system can be captured by O_2 molecules to form superoxide radicals ($O_2^{\bullet-}$), H_2O reacts with holes (h^+) to generate $^{\bullet}OH$ radicals, both of which have strong oxidizing ability and can degrade organic dyes.

In summary, the composite of kaolinite and ferrite nanoparticles with spinel structure can not only improve the adsorption capacity of kaolinite, but also effectively separate photogenerated electrons and holes, and increase reactive sites. In addition, Ag nanoparticles in Ag/kaolinite materials can act as electron acceptors to store electrons. Due to the Schottky barrier, the separation of incoming electron-hole pairs is enhanced. Moreover, Ag nanoparticles can use the SPR effect to form a local electromagnetic field, which can generate active free radicals.

4. Application of kaolinite-based photocatalysts

Researchers have focused on semiconductor photocatalysis in recent decades because it can solve the increasingly serious environmental pollution and energy crisis issues to some extent by using inexhaustible sunlight and avoiding secondary pollution [119]. As mentioned above, an ideal excellent semiconductor photocatalyst should have (a) excellent light absorption capacity, that is, a narrow bandgap and a high absorption coefficient; (b) high efficiency of photo-generated electron-hole pair separation; (c) long-term stability and reusability. P25 is a highly dispersed gas phase nanometer titanium dioxide produced by Evonik Degussa using the method of preparing ultrafine particle oxide by high temperature hydrolysis. It has broad application prospects in the fields of environment, information, materials, energy, medical and health [120]. However, it can only absorb ultraviolet light and cannot be reused, which limits its application [121]. Loading natural kaolinite can improve the photocatalytic efficiency. It can not only maintain the photocatalytic activity of the catalyst but also promote the rapid adsorption of pollutants on the surface of the composite photocatalyst. In this section, various photocatalytic applications of the kaolinite based photocatalysts are briefly summarized.

4.1. Photocatalytic hydrogen evolution

Theoretically, semiconductors with suitable CB and VB positions can be used as photocatalysts to complete photocatalytic oxygen release reactions and hydrogen evolution reactions [122]. However, the complex oxygen evolution process is a four-electron process, and few articles have reported it.

In order to solve the problems of energy consumption and environmental pollution caused by fossil fuels such as petroleum and coal, hydrogen energy has gradually attracted widespread attention due to its clean pollution-free cleanliness [84]. Semiconductor photocatalysis technology can draw widespread attention by using inexhaustible solar energy to split water into hydrogen [123]. To effectively promote water decomposition, the CB minimum edge of the photocatalyst should be less than the H^+/H_2 reduction potential (0 V *vs.* NHE), and the VB maximum edge should be greater than the H_2O/O_2 oxidation potential (+1.23 V *vs.* NHE) [124]. Theoretically, the use of g-C_3N_4 as a photocatalyst can complete the hydrogen evolution reaction of water decomposition due to its proper CB and VB positions. Meanwhile, building a strong coupling between the semiconductor photocatalyst and a suitable co-catalyst is conducive to the photocatalytic hydrogen evolution reaction. The cocatalyst can act as an electron absorber to promote charge separation and reduce the activation energy or overpotential of the catalytic reaction. To date, the precious metal platinum has proved to be the most effective cocatalyst for hydrogen evolution. The excellent co-catalytic performance promoted by the plasma coupling effect is of course widely used in semiconductor photocatalytic systems [125]. For example, the composite material of nano-g-C_3N_4 and meta-kaolinite was successfully synthesized by a simple method of directly calcining the mixture of melamine and kaolinite [50]. The as-prepared meta-kaolinite/g-C_3N_4-70.4% exhibited a favorable hydrogen evolution rate of 288 $\mu mol\ g^{-1}\ h^{-1}$, which was much higher than that for any other existing pure g-C_3N_4 photocatalyst. The probable mechanism of photocatalytic H_2 evolution on meta-kaolinite/g-C_3N_4 composites is shown in Fig. 6. The improvement of the activity of the photocatalytic hydrogen evolution reaction is attributed to the electronegativity of meta-kaolinite and the nanometerization of g-C_3N_4. Reducing the thickness of the g-C_3N_4 nanoplates may increase the surface area, thereby increasing the number of active sites [126]. The feasibility of interfacial redox reaction plays an important role in hydrogen evolution during photocatalytic water decomposition. Moreover, in order to better expand the light absorption and increase the reactive site, making defective porous structure g-C_3N_4 is an effective method [28]. The growth restricted on the porous kaolinite-derived template to produce porous g-C_3N_4 with edge site defects exhibits excellent photocatalytic activity. The results show that under visible light irradiation, the PHE rate of porous g-C_3N_4 reaches 1917 $\mu mol\ g^{-1}\ h^{-1}$, which is 2.37 times that of g-C_3N_4. The formation of the porous structure can not only increase the surface area, but also provide mass diffusion channels, expanded light absorption and defects, and act as active sites for mediating pores to the interface oxidation reactivity.

In summary, kaolinite-based photocatalysts are considered to be a viable alternative method for hydrogen production with visible light irradiation with the aid of cocatalysts. However, the noble metal promoters are very expensive, which limits the application of photocatalysts. Therefore, the ideal method is to use high-efficiency photocatalysts and non-precious metal co-catalysts to achieve an economical clean energy production system.

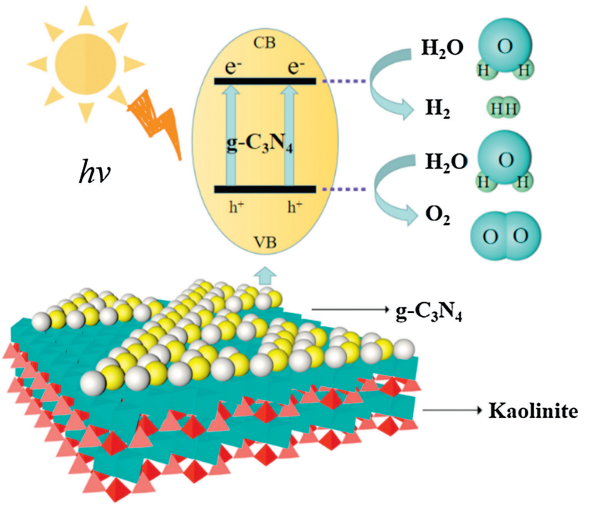

Fig. 6. Schematic mechanism of photocatalytic H_2 evolution on kaolinite/g-C_3N_4 composite.

4.2. Photocatalytic removal of environmental pollutants

Traditional wastewater treatment methods, such as biological treatment, filtration, and adsorption, have some disadvantages, such as high cost, low efficiency, and non-recyclability [127]. Semiconductor photocatalysts degrade various pollutants in wastewater through a series of redox reactions under light, which is a promising wastewater treatment technology [6]. In this sense, composite photocatalytic materials such as TiO_2, g-C_3N_4 and other photocatalytic materials anchored in kaolinite structure can not only use solar energy to degrade pollutants through redox reaction, but also increase photocatalytic activity [122,128].

Kaolinite is a new development direction in the field of environmental purification due to its excellent adsorption as a carrier for semiconductor-based photocatalysts. Recently, TiO_2 nanoparticles and C_3N_4 nanosheets were coloaded on kaolinite by Niu *et al.* [53] for degradation of MB dye. The composite material showed an extremely high degradation rate, which was 18.8 and 24.7 times higher than that of pure TiO_2 and C_3N_4, respectively. In order to solve the difficulty of natural clay minerals to participate in the separation and transfer of charge carriers in the photocatalytic system, natural iron-rich kaolinite clay was used as a multifunctional carrier to construct a cadmium sulfide (CdS) composite photocatalyst by Jiang *et al.* [129] for degradation of methyl orange (MO) aqueous solution. The photocatalytic activity of CdS/kaolinite composites was 2.6 times higher than that of pure CdS nanoparticles, and it retained nearly 80% of the photocatalytic activity after two cycles. The composite material provided an oxygen-enriched microenvironment on its surface through its strong hydroxyl oxygen adsorption capacity, and then promoted the reaction of CdS nanoparticles, thereby improving the photocatalytic performance.

It should be noted that compared with pure semiconductor catalysts, the kaolinite-based Z-scheme heterojunction photocatalyst exhibits excellent photocatalytic activity for the degradation of organic pollutants. For instance, the decomposition of MO and methylene blue (MB) was very limited with pure catalyst, whereas it was efficient with the Z-type heterojunction of kaolinite/TiO_2/g-C_3N_4 [53] and BiOCl/g-C_3N_4/kaolinite [4]. Other work has indicated the Kaolinite/TiO_2/cobalt(II) [48]. Z-scheme heterojunction showed its universality for the degradation of organic pollutants trimethoprim, caffeine and prometryn. As we all know, photogenerated holes (h^+), hydroxyl radicals ($^{\bullet}OH$) and superoxide anion radicals ($O_2^{\bullet-}$) are the main reactive species for oxidizing organic pollutants during the photocatalytic reaction. However, the insufficient oxidation ability of pure semiconductors cannot drive the oxidation process of H_2O to generate $^{\bullet}OH$. Perversely, in a Z-type heterojunction such as kaolinite/TiO_2/g-C_3N_4 [52], photogenerated electrons remain in the CB of g-C_3N_4 while holes remain in the VB of the TiO_2, which not only suppresses photogeneration the electron-hole recombination prolongs the life of photogenerated carriers, and also retains the strong reduction and oxidation ability of photogenerated electrons and holes. Therefore, the kaolinite-based Z scheme heterojunction composite photocatalyst not in terms with high space charge separation efficiency, but also has excellent redox properties, and is a valuable photocatalyst in the field of degradation of organic pollutants.

4.3. Photocatalytic CO_2 reduction

The increasing depletion of non-renewable fossil fuels and existing resources is increasing research and development of alternative energy sources [130]. In addition to photocatalytic hydrogen production, the use of semiconductor photocatalysts to reduce CO_2 light to hydrocarbon fuels has been regarded as an optional technology to solve the problem of energy depletion, and will also reduce the greenhouse effect [131,132]. As shown in reactions 22–26 [130], CO_2 reduction is converted to formic acid, carbon monoxide, methane, methane and methanol by multi-electron transfer, respectively.

$$CO_2 + 2H^+ + 2e^- \rightarrow HCOOH \quad E^0_{redox} = -0.61\ V \tag{14}$$

$$CO_2 + 2H^+ + 2e^- \rightarrow CO + H_2O \quad E^0_{redox} = -0.53\ V \tag{15}$$

$$CO_2 + 4H^+ + 4e^- \rightarrow HCHO + H_2O \quad E^0_{redox} = -0.48\ V \tag{16}$$

$$CO_2 + 6H^+ + 6e^- \rightarrow CH_3OH + H_2O \quad E^0_{redox} = -0.38\ V \tag{17}$$

$$CO_2 + 8H^+ + 8e^- \rightarrow CH_4 + 2H_2O \quad E^0_{redox} = -0.24\ V \tag{18}$$

TiO_2 can be used as a potential candidate for driving the photocatalytic reaction of CO_2 reduction due to high efficiency and non-toxicity. Kaolinite can effectively prevent TiO_2 from forming particle aggregates and act as a fixing agent, thereby improving the effective surface area and photocatalytic efficiency. The kaolinite/TiO_2 composite for photocatalytic reduction of CO_2 was prepared by Kočí *et al.* [67] using thermal hydrolysis of kaolinite/titanyl sulphate suspension. Compared with the traditional commercial catalyst P25, the results show that loading kaolinite on TiO_2 can improve the performance of TiO_2, and significantly improve the yield of methane and methanol, the products of CO_2 photocatalytic reduction. The introduction of TiO_2 nanoparticles into the kaolinite structure leads to a decrease in anatase grain size, an increase in surface area and pore volume, and avoids the formation of TiO_2 aggregates in suspension. Kaolinite can change the acidity and alkalinity of the catalyst surface, inhibit the recombination of electron-hole pairs, and increase the photocatalytic activity.

The foregoing work shows that the combination of kaolinite-based photocatalyst and cocatalyst can significantly improve the photocatalytic efficiency of CO_2 reduction. However, current research is greatly limited due to the stability of the material and the cost of the co-catalyst. Expected to require long-term effort to promote the practical application of the CO_2 reduction photocatalytic system and the development of non-precious metal promoters.

4.4. Photocatalytic disinfection

Aqueous antibiotics and aquatic bacteria are considered to be the main categories of water pollutants due to their ubiquitous nature that poses a threat to global public health [133]. Therefore, some safe and efficient methods are needed to purify bacteria and viruses. Photocatalytic disinfection has proven to be a superior method compared to traditional disinfection methods (such as chlorination and ultraviolet disinfection) due to its non-toxic, efficient and stable advantages [134].

Recent studies have demonstrated that kaolinite-based photocatalysts exhibit antibacterial activity under visible light irradiation. For instance, nano TiO_2 can interact with bacteria, viruses or

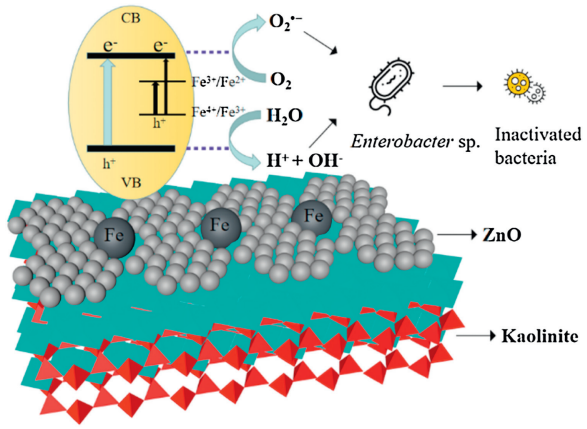

Fig. 7. The photocatalytic disinfection of *Enterobacter* sp. using ZnO/kaolinite under visible light.

algae under ultraviolet radiation [135], the composites kaolinite/TiO_2 were prepared through drying at 105 °C and calcining at 600 °C [136]. Kaolinite/TiO_2 samples have obvious antibacterial activity against four human pathogenic bacterial strains (*Staphylococcus aureus*, *E. coli*, *Enterococcus faecalis*, *Pseudomonas aeruginosa*). Compared with pure photocatalyst, kaolinite/TiO_2/g-C_3N_4 prepared by mild sol-gel method has enhanced adsorption-photocatalytic degradation ability of ciprofloxacin (CIP) under visible light irradiation. The degradation efficiency of the composite materials is bare TiO_2, the apparent rate constants of g-C_3N_4 and P25 are about 5.35 times, 6.35 times and 4.49 times, respectively. Meanwhile, there are some difficulties in using bare ZnO for photocatalytic disinfection, such as the aggregation of nanoparticles, crystal growth or surface morphology changes, which will eventually reduce its catalytic performance and limit its commercial application. The combination of ZnO and kaolinite catalyst can solve these problems to a certain extent. For instance, ZnO/kaolinite was synthesized by co-precipitation technique through using Fe-doped ZnO nanoparticles impregnated on Kaolinite [30]. The results show that $O_2^{\bullet-}$ (Fig. 7) plays a key role in disinfecting the bacteria of the *Enterobacter* genus. Compared with conventional catalysts (such as g-C_3N_4 and ZnO), kaolinite/ZnO also exhibits excellent efficiency, stability and reusability.

The above examples show that the kaolinite-based photocatalyst has good antibacterial activity under visible light irradiation. However, the research on bacterial disinfection is related to human health and safety. Moreover, the research on photocatalysis technology is at an initial stage, and more effort needs to be invested in the photocatalytic disinfection research based on kaolinite-based photocatalysts.

5. Conclusions

Kaolinite is a promising photocatalytically-supported substance due to its unique interlayer space as well as low-cost, non-toxic, environmentally friendly, stability and other advantages. We briefly analyze the research history, current status, and development trends of photocatalysts. The crystal structure, chemical composition and physical and chemical properties of kaolinite are expounded. A large number of studies have shown that kaolinite-based photocatalysts have excellent catalytic activity, and the performance of various catalysts are discussed in detail. The internal function and catalytic mechanism of kaolinite as carrier and different catalysts (TiO_2, g-C_3N_4, ZnO) were analyzed. The synergistic effects of natural kaolinite in composite materials include: (a) Promote the dispersion of semiconductor nanoparticles, effectively avoid particle agglomeration and increase the specific surface area; (b) enhance the absorption capacity of composite materials, effectively increase the contact probability of pollutants and composite surface active ingredients; (c) the electrostatic force on the surface of kaolinite and a large number of negative hydroxyl groups can effectively promote the rapid separation of photogenerated carriers; (d) due to the large size and high specific gravity of kaolinite, the composite material can be easily recycled, thus retaining the reusability of the catalyst, and anchoring the semiconductor on the surface, reducing the environmental risk of nanoparticle diffusion. Although some encouraging results have been reported so far, the research on kaolinite photocatalytic materials is still in the preliminary stage and needs further improvement. In particular, the modification of kaolinite-based photocatalysts is difficult, the utilization rate of visible light is low, and the photocatalytic efficiency is relatively low, which limits its application in industrial practice.

Therefore, in order to obtain a high and low-cost photocatalytic system, the performance of kaolinite-based photocatalysts needs to be further improved. Notably, most of the current researches focus on the combination of kaolinite and traditional semiconductors (such as TiO_2, g-C_3N_4, ZnO), future research can try to combine kaolinite with new semiconductors. For example, it is possible to develop an inexpensive co-catalyst that does not contain precious metals to be applied to kaolinite-based photocatalysts to ensure efficiency while controlling costs to achieve industrial applications. In terms of experiment work, optimize the method of kaolinite intercalation modification, and change the layered structure of kaolinite under economical and technically feasible conditions to be suitable for loading different semiconductor nanoparticles and improve the photocatalytic efficiency. A comprehensive and in-depth understanding of the photocatalytic mechanism of composite materials helps to synthesize excellent photocatalytic materials. Therefore, it is necessary to study the energy band structure of the kaolinite photocatalyst based on the first-principles DFT calculation, and the effective separation mechanism of the photogenerated carriers. In terms of experimental content and data processing, the integration and enrichment process between kaolinite and catalyst should be further explored, and the mechanism of pollutant migration and transfer in the photocatalytic system should be studied. Therefore, it is necessary to combine experiments with computer models to jointly promote the development of the field. So that the kaolinite photocatalyst can play a greater role in practical applications.

Declaration of competing interest

All authors declared that they do not have any commercial or associative interest that represents a conflict of interest in connection with the work submitted.

Acknowledgments

The authors gratefully acknowledge the financial support provided by the Science and Technology Major Projects of Shanxi Province of China (No. 20181101003) and Special Funds for Basic Scientific Research of Central Colleges (No. 300102299306, 300102299304).

References

[1] Q. Wang, M. Su, R.R. Li, P. Ponce, J. Clean. Prod. 225 (2019) 1017–1032.
[2] C. Zhang, G.M. Zeng, D.L. Huang, et al., Chem. Eng. J. 373 (2019) 902–922.
[3] H.B. Lu, X.M. Liu, F. Liu, et al., Appl. Catal. B: Environ. 250 (2019) 1–9.

[4] X.B. Dong, Z.M. Sun, X.W. Zhang, C.Q. Li, S.L. Zheng, J. Taiwan Inst. Chem. E 84 (2018) 203–211.
[5] Y.R. Song, X. Xin, S.H. Guo, et al., Chem. Eng. J. 384 (2020) 123337.
[6] Z. Sun, F. Yuan, X. Li, et al., Minerals-Basel 8 (2018) 437.
[7] K. Li, X. An, K.H. Park, M. Khraisheh, J. Tang, Catal. Today 224 (2014) 3–12.
[8] H. Zhang, J. He, C. Zhai, M. Zhu, Chin. Chem. Lett. 30 (2019) 2338–2342.
[9] D.Y. He, Z.C. Zhang, Y. Xing, et al., Chem. Eng. J. 384 (2020) 123258.
[10] A.F.K. Honda, Nature 238 (1972) 37–38.
[11] F.T. Yi, J.Q. Ma, C.W. Lin, et al., J. Alloys Compd. 821 (2020) 153557.
[12] S. Hu, Y. Yu, Y. Guan, et al., Chin. Chem. Lett. 31 (2020) 2839–2842.
[13] X. Deng, Y. Chen, J. Wen, et al., Sci. Bull. 65 (2020) 105–112.
[14] M. Xu, Y. Chen, J. Qin, et al., Environ. Sci. Technol. 52 (2018) 13879–13886.
[15] P. Guan, H.Y. Bai, F.G. Wang, et al., Chem. Eng. J. 358 (2019) 658–665.
[16] H.D. She, Y.D. Sun, S.P. Li, et al., Appl. Catal. B: Environ. 245 (2019) 439–447.
[17] C.Y. Zhai, M.J. Sun, L.X. Zeng, et al., Appl. Catal. B: Environ. 243 (2019) 283–293.
[18] Y. Li, X.Y. Wu, J. Li, K. Wang, G.K. Zhang, Appl. Catal. B: Environ. 229 (2018) 218–226.
[19] C.J. Wang, Y.L. Zhao, H. Xu, et al., Appl. Catal. B: Environ. 263 (2020) 118314.
[20] J.D. Lopes, W.V. Rodrigues, V.V. Oliveira, et al., Appl. Clay Sci. 168 (2019) 295–303.
[21] G.N. Shao, M. Engole, S.M. Imran, S.J. Jeon, H.T. Kim, Appl. Surf. Sci. 331 (2015) 98–107.
[22] G.X. Zhang, Y.Y. Liu, S.L. Zheng, Z. Hashisho, J. Hazard. Mater. 364 (2019) 317–324.
[23] J.d.S. Lopes, W.V. Rodrigues, V.V. Oliveira, et al., Appl. Clay Sci. 168 (2019) 295–303.
[24] P. Szabó, B. Zsirka, D. Fertig, et al., Catal. Today 287 (2017) 37–44.
[25] B. Pan, X. Yin, S. Iglauer, Adv. Colloid Interface Sci. 285 (2020) 102266.
[26] A.C. Wu, D.X. Wang, C. Wei, et al., Appl. Clay Sci. 183 (2019) 105352.
[27] R. Portela, I. Jansson, S. Suarez, et al., Chem. Eng. J. 310 (2017) 560–570.
[28] Z. Zhang, L. Lu, Z. Lv, et al., Appl. Catal. B: Environ. 232 (2018) 384–390.
[29] Y. Zhang, H. Gan, G. Zhang, Chem. Eng. J. 172 (2011) 936–943.
[30] A.J. Misra, S. Das, A.P. Habeeb Rahman, et al., J. Colloid Interface Sci. 530 (2018) 610–623.
[31] V.B. Yadav, R. Gadi, S. Kalra, J. Environ. Manage. 232 (2019) 803–817.
[32] B. Ren, F.F. Min, L.Y. Liu, et al., Appl. Surf. Sci. 504 (2020) 144324.
[33] G.B. Chen, X. Li, L. Zhou, S.W. Xia, L.M. Yu, Appl. Surf. Sci. 488 (2019) 494–502.
[34] Suhartana, A.A. Janitra, C. Aziniyawati, A. Darmawan, IOP Conf. Ser.: Mater. Sci. Eng. 509 (2019) 012140.
[35] A.A. Baba, M.A. Raji, A.Y. Abdulkareem, et al., Mining Metall Explor. 36 (2019) 1091–1099.
[36] V. Vagvolgyi, K. Gyorfi, B. Zsirka, E. Horvath, J. Kristof, J. Therm. Anal. Calorim. 142 (2020) 289–299.
[37] A.H. Zyoud, T. Zorba, M. Helal, et al., Int. J. Environ. Sci. Technol. 16 (2019) 6267–6276.
[38] O.K. Kim, L.D. Volkova, N.A. Zakarina, A.R. Brodskii, Chem. Technol. Fuels Oils 55 (2019) 378–388.
[39] A. Alshameri, H.P. He, J.X. Zhu, et al., Appl. Clay Sci. 159 (2018) 83–93.
[40] K. Mamulova Kutlakova, J. Tokarsky, P. Kovar, et al., J. Hazard. Mater. 188 (2011) 212–220.
[41] X.Y. Li, J. Ouyang, Y.H. Zhou, H.M. Yang, Sci. Rep. 5 (2015) 13763.
[42] R.B. Zhao, X. Zhang, Y.G. Su, Z.L. Liu, C.F. Du, Chem. Eng. J. 380 (2020) 122432.
[43] Q. Zhang, Z.L. Yan, J. Ouyang, et al., Appl. Clay Sci. 157 (2018) 283–290.
[44] D.H. Jiang, Z.R. Liu, L.J. Fu, H.H. Jing, H.M. Yang, J. Phys. Chem. C 122 (2018) 25900–25908.
[45] T.H. Sia, S. Dai, B. Jin, M. Biggs, M.N. Chong, Chem. Eng. J. 279 (2015) 939–947.
[46] X. Li, K. Peng, H. Chen, Z. Wang, Sci. Rep. 8 (2018) 11663.
[47] H. Xu, S. Sun, S. Jiang, et al., J. Sol-Gel Sci. Technol. 87 (2018) 676–684.
[48] T.H. da Silva, A.O. Ribeiro, E.J. Nassar, et al., J. Braz. Chem. Soc. 30 (2019) 2610–2623.
[50] X. Wang, Z. Zhao, Z. Shu, et al., Appl. Clay Sci. 166 (2018) 80–87.
[51] Q.H. Zhao, L.J. Fu, D.H. Jiang, Y.F. Xi, H.M. Yang, Chem. Commun. 54 (2018) 8249–8252.
[52] C. Li, Z. Sun, W. Zhang, C. Yu, S. Zheng, Appl. Catal. B: Environ. 220 (2018) 272–282.
[53] J. Niu, A. Wu, D. Wang, et al., Mater. Lett. 230 (2018) 32–35.
[54] K. Mamulová Kutláková, J. Tokarský, P. Peikertová, Appl. Catal. B: Environ. 162 (2015) 392–400.
[55] H. Xu, E. Fan, J. Liu, et al., Appl. Clay Sci. 181 (2019) 105241.
[56] Z. Li, N. Potter, J. Rasmussen, J. Weng, G. Lv, Chemosphere 202 (2018) 127–135.
[57] X. Dong, B. Ren, Z. Sun, et al., Appl. Catal. B: Environ. 253 (2019) 206–217.
[58] P. Tun, K. Wang, H. Naing, J. Wang, G. Zhang, Appl. Clay Sci. 175 (2019) 76–85.
[59] Y.J. Li, Z.H. Yin, G.R. Ji, et al., Appl. Catal. B: Environ. 246 (2019) 12–20.
[60] Z.L. Ma, J.C. Liu, Y.F. Zhu, et al., J. Alloys Compd. 822 (2020) 153553.
[61] Y. Li, Y. Fu, M. Zhu, Appl. Catal. B: Environ. 260 (2020) 118149.
[62] N. Seydi, B. Mahdavi, S. Paydarfard, et al., Appl. Organomet. Chem. 33 (2019) e5009.
[63] A. Giampiccolo, D.M. Tobaldi, S.G. Leonardi, et al., Appl. Catal. B: Environ. 243 (2019) 183–194.
[64] C.M. Gao, T. Wei, Y.Y. Zhang, et al., Adv. Mater. 31 (2019) 1806596.
[65] Y. Zhang, C.W. Foster, C.E. Banks, et al., Adv. Mater. 28 (2016) 9391–9399.
[66] F. Qi, W.J. An, H. Wang, et al., Mater. Sci. Semicond. Process. 109 (2020) 104954.
[67] K. Kočí, V. Matějka, P. Kovář, Z. Lacný, L. Obalová, Catal. Today 161 (2011) 105–109.
[68] C.Q. Li, Z.M. Sun, X.B. Dong, S.L. Zheng, D.D. Dionysiou, J. Catal. 367 (2018) 126–138.
[69] L.D. Mora, L.F. Bonfim, L.V. Barbosa, et al., Materials 12 (2019) 3943.
[70] C. Wang, H.S. Shi, P. Zhang, Y. Li, Appl. Clay Sci. 53 (2011) 646–649.
[71] D.H. Jiang, Z.R. Liu, L.J. Fu, H.M. Yang, ACS Appl. Mater. Interfaces 12 (2020) 9872–9880.
[72] K. Pinato, K. Suttiponparnit, S. Jinawath, D.P. Kashima, J. Mater. Sci. 55 (2020) 1451–1463.
[73] Y. Han, S. Zhao, H. Wu, S. Asuha, Desalin. Water Treat. 160 (2019) 240–249.
[74] A. Vali, H.Z. Malayeri, M. Azizi, H. Choi, Appl. Catal. B: Environ. 266 (2020) 118646.
[75] Y.X. Zhao, Y.F. Zhao, R. Shi, et al., Adv. Mater. 31 (2019) 1806482.
[76] K. Chen, C.L. Chen, X.M. Ren, A. Alsaedi, T. Hayat, Chem. Eng. J. 359 (2019) 944–954.
[77] B. Babu, R. Koutavarapu, J. Shim, K. Yoo, Sep. Purif. Technol. 240 (2020) 116652.
[78] V. Hasija, P. Raizada, A. Sudhaik, et al., Appl. Mater. Today 15 (2019) 494–524.
[79] X. Wang, K. Maeda, A. Thomas, et al., Nat. Mater. 8 (2009) 76–80.
[80] S. Wang, P. He, L.P. Jia, et al., Appl. Catal. B: Environ. 243 (2019) 463–469.
[81] A. Bafaqeer, M. Tahir, N.A.S. Amin, Appl. Catal B: Environ. 242 (2019) 312–326.
[82] N.A. Mohamed, J. Safaei, A.F. Ismail, et al., J. Alloys Compd. 818 (2020) 152916.
[83] Y.X. Zeng, H. Li, J.M. Luo, et al., Appl. Catal. B: Environ. 249 (2019) 275–281.
[84] C.X. Zhao, Z.P. Chen, J.S. Xu, et al., Appl. Catal. B: Environ. 256 (2019) 117867.
[85] Z.J. Luo, Y.Y. Song, M.J. Wang, et al., J. Photochem. Photobiol. A 389 (2020) 112241.
[86] B. He, Y. Du, Y.B. Feng, et al., Appl. Surf. Sci. 506 (2020) 145031.
[87] K.L. He, J. Xie, M.L. Li, X. Li, Appl. Surf. Sci. 430 (2018) 208–217.
[88] Y.J. Zhou, L.X. Zhang, J.J. Liu, et al., J. Mater. Chem. A 3 (2015) 3862–3867.
[89] M. Hojamberdiev, M.M. Khan, Z. Kadirova, et al., Renew. Energy 138 (2019) 434–444.
[90] Z.M. Sun, G.Y. Yao, X.Y. Zhang, S.L. Zheng, R.L. Frost, Appl. Clay Sci. 129 (2016) 7–14.
[91] Z.M. Sun, C.Q. Li, X. Du, S.L. Zheng, G.F. Wang, J. Colloid Interface Sci. 511 (2018) 268–276.
[92] M. Raji, A.E. Qaiss, R. Bouhfid, RSC Adv. 10 (2020) 4916–4926.
[93] N.I.M. Rosli, S.M. Lam, J.C. Sin, A.R. Mohamed, Mater. Lett. 261 (2020) 126990.
[94] F. Guo, M.Y. Li, H.J. Ren, et al., Sep. Purif. Technol. 228 (2019) 115770.
[95] S.W. Cao, J.X. Low, J.G. Yu, M. Jaroniec, Adv. Mater. 27 (2015) 2150–2176.
[96] M. Chen, C.S. Guo, S. Hou, et al., Appl. Catal. B: Environ 266 (2020) 118614.
[97] S. Lee, J. Kim, I. Kim, et al., Environ. Geochem. Health 41 (2019) 2011–2021.
[98] S.F. Kang, M.F. He, M.Y. Chen, et al., Carbon 159 (2020) 51–64.
[99] S.J. Armakovic, M. Grujic-Brojcin, M. Scepanovic, et al., Arab J. Chem. 12 (2019) 5355–5369.
[100] I. Ali, S. Park, J.O. Kim, J. Alloys Compd. 821 (2020) 153498.
[101] J.Q. Pan, Z.J. Dong, B.B. Wang, et al., Appl. Catal. B: Environ. 242 (2019) 92–99.
[102] Y. Huo, Y. Yang, K. Dai, J.F. Zhang, Appl. Surf. Sci. 481 (2019) 1260–1269.
[103] N. Fajrina, M. Tahir, Appl. Surf. Sci. 471 (2019) 1053–1064.
[104] X.J. Zhou, C.L. Shao, X.H. Li, et al., J. Hazard. Mater. 344 (2018) 113–122.
[105] J.Y. Tian, Q. Shao, J.K. Zhao, et al., J. Colloid Interface Sci. 541 (2019) 18–29.
[106] N. Fajrina, M. Tahir, Int. J. Hydrogen Energy 45 (2020) 4355–4375.
[107] J.A. Mbey, F. Thomas, Carbohydr. Polym. 117 (2015) 739–745.
[108] X. Jin, D.D. Wu, J.Y. Ling, et al., Environ. Sci. Technol. 53 (2019) 10645–10653.
[109] K. Rabe, L.F. Liu, N.A. Nahyoon, et al., J. Taiwan Inst. Chem. E 96 (2019) 463–472.
[110] Y. Bao, L. Gao, C. Feng, J. Ma, S. Lyu, Mater. Sci. Eng. B: Adv. 263 (2021) 114887.
[111] S. Rao, G.S. Shekhawat, J. Environ. Chem. Eng. 2 (2014) 105–114.
[112] M.R. Abukhadra, A. Helmy, M.F. Sharaf, et al., J. Environ. Manage. 271 (2020) 111019.
[113] W. Wang, X. Wang, L. Gan, et al., J. Mater. Sci. Technol. 77 (2021) 117–125.
[114] J. Wen, L. Ling, Y. Chen, Z. Bian, Chin. J. Catal. 41 (2020) 1674–1681.
[115] D. Mohanty, S.K. Satpathy, B. Behera, R.K. Mohapatra, Mater. Today 33 (2020) 5226–5231.
[116] S.J. Olusegun, N.D.S. Mohallem, Environ. Pollut. 260 (2020) 114019.
[117] L. Ling, Y. Feng, H. Li, et al., Appl. Surf. Sci. 483 (2019) 772–778.
[118] Z. Sun, X. Zhang, X. Dong, et al., J. Materiomics 6 (2020) 582–592.
[119] R. Ma, S. Zhang, T. Wen, et al., Catal. Today 335 (2019) 20–30.
[120] L.H. Yu, X.Y. Zhang, G.W. Li, et al., Appl. Catal. B: Environ. 187 (2016) 301–309.
[121] M.G. Mendez-Medrano, E. Kowalska, A. Lehoux, et al., J. Phys. Chem. C 120 (2016) 5143–5154.
[122] Y. Feng, M. Xu, H. Liu, W. Li, H. Li, Z. Bian, Nano Energy 73 (2020) 104768.
[123] H. Tang, R. Wang, C.X. Zhao, et al., Chem. Eng. J. 374 (2019) 1064–1075.
[124] X.L. Yin, L.L. Li, M.L. Liu, et al., Chem. Eng. J. 370 (2019) 305–313.
[125] H.N. Che, G.B. Che, P.J. Zhou, et al., Chem. Eng. J. 382 (2020) 122870.
[126] L. Cui, S.L. Liu, F.K. Wang, et al., J. Alloys Compd. 826 (2020) 154001.
[127] W.P. Xiong, Z.T. Zeng, G.M. Zeng, et al., Chem. Eng. J. 374 (2019) 91–99.
[128] Z.Q. Chen, P.F. Chen, P.X. Xing, et al., Fuel 241 (2019) 1–11.
[129] D. Jiang, Z. Liu, L. Fu, H. Jing, H. Yang, J. Phys. Chem. C 122 (2018) 25900–25908.
[130] O. Ola, M.M. Maroto-Valer, J. Photochem. Photobiol. C 24 (2015) 16–42.
[131] L. Hao, L. Kang, H.W. Huang, et al., Adv. Mater. 31 (2019) 1900546.
[132] K.R. Reddy, C.V. Reddy, M.N. Nadagouda, et al., J. Environ. Manage. 238 (2019) 25–40.
[133] P.J. Landrigan, R. Fuller, S. Fisher, et al., Sci. Total Environ. 650 (2019) 2389–2394.
[134] P. Raizada, A. Sudhaik, P. Singh, et al., Sep. Purif. Technol. 212 (2019) 887–900.
[135] X.Y. Ma, Q.J. Xiang, Y.L. Liao, T.L. Wen, H.W. Zhang, Appl. Surf. Sci. 457 (2018) 846–855.
[136] K. Dedkova, K. Matejova, J. Lang, et al., J. Photochem. Photobiol. B 135 (2014) 17–22.